View metadata, citation and similar papers at core.ac.uk
brought to you by CORE
provided by UPCommons. Portal del coneixement obert de la UPC

Model Calibration for Leak Localization, a Real Application

Gerard Sanz [1], Jordi Meseguer [2], Ramon Pérez [3]
[1,3] SAC-UPC, Rambla Sant Nebridi 10, Terrassa 08222, Catalunya.
[2] Cetaqua, Water Technology Center
[3] *ramon.perez@upc.edu*

ABSTRACT

The localization of leaks in Water Distribution Networks has a major relevance in terms of environmental and economic efficiency. This localization is generally carried on in situ by human operators using time consuming methods like acoustic loggers. Nevertheless, the automated aid provided to the operators is continuously increasing thanks to the exhaustive use of models. Models that have to be calibrated and updated in order to provide proper help and an improvement in the leak search. This paper presents an experience of leak localization using steady state models combined with a demand calibration algorithm. The calibration produces a notable improvement of the localization accuracy and signals changes in the network configuration. Results presented are based on real data and a real leak provoked for the test.

Keywords: Leak localization, calibration, water networks, demands, pressure measurements

1 INTRODUCTION AND PROBLEM STATEMENT

Leakage in water distribution systems has attracted a lot of attention by both practitioners and researchers over the past years. [10] provides a review of leakage management related methods in distribution pipe systems from detection and assessment to efficient control. Leak localization techniques can be divided into two categories: external and internal. The use of external methods like acoustic logging, penetrating radar or liquid detection methods has some drawbacks like needing a large number of sensors, not being suitable for application in large urban areas, or being invasive. On the other hand, internal methods use continuously monitored data to infer the position of leaks. The supervision of huge complex systems like water distribution networks (WDN) requires a lot of data unless the knowledge of the system is well-organised in a model. Data driven methods [14] relay on the information provided by the sensors, thus the conclusions extracted are limited to the level where enough information comes. Many techniques based on transient analysis can be found in literature [15]. Non-transient model-based leakage localization techniques have been also developed during the last years [7]. These techniques analyse the difference between measurements and estimated values from leaky scenarios to signal the probability of a zone to contain leakage.

A good calibration of the models is required to obtain reliable results when using them [13]. [12] thoroughly reviewed the state of the art of the global calibration problem. Generally, the inverse problem has to be solved using field measurements to adjust the network parameters. Least squares [3] and evolutionary methods [4] are the most used automatic calibration techniques for WDN models. Once the model is calibrated, the model-based leak detection and localization methodologies can make use of it. However, these methodologies do not consider the evolution of demands in the real system. This evolution should be taken into account because demands are parameters that change continuously and leakages may be masked with their evolution.

The method used in this work [8] is based on the computation of the correlation between measurements and estimated values from leaky scenarios, signalling the network area where high correlations are obtained. In the past, this method has already been satisfactory tested in a real leak scenario, with a location accuracy of 180 metres in a 3 km^2 network using 5 pressure sensors [7].

In next subsection the case study and the problem statement are presented. In section 2 both methodologies, calibration and leak localisation, are described. Their results are presented in section 3. Finally, conclusions are discussed in section 4.

1.1 Case Study

In the work described in this paper, the leakage localisation methodology is applied to a district metered area (DMA) composed of 5153 pipes and 4991 junctions. Pressure and flow are monitored at both water inlets with a sample time of 10 min. The resolution is 0.3 l/s for the flow sensors, and 0.1 mwc for the pressure sensors. The minimum night flow is of about 45 l/s, and the peak-hour flow is 85 l/s. In the EFFINET project[1], this DMA has been equipped with 6 new inner pressure sensors (green stars in Figure 1) applying the optimal sensor placement method described in [1]. These sensors have been deployed to enhance the performance of the leakage localization method described in Section 2.1.

Figure 1. Water network of Castelldefels Platja DMA (EPANET model) highlighting inner pressure sensors (green stars), DMA inlets (red triangles) and localization of the real tested leak (red circle).

The tested real leak scenario was scheduled in the week starting the 28th of September 2015 and lasting 5 days. The water utility technicians opened a discharge valve on September 29th closing it the 1st of October. The real leak was located at the red circle shown in Figure 1 having an average size of almost 5 l/s, although this information was unknown by the people running the leakage localization algorithms.

2 METHODOLOGY

The two methodologies are described briefly in this section. For more detailed information there are references to our previous works.

2.1 Model Calibration

The demand model based on distributing the total inflow all over the nodes depending on billing cannot explain the daily variation in the relative pressure behaviour between two areas in the

[1] Grant FP7-ICT-2012-318556 of the European Commission

network. The demand model in equation 2.1.1 presents a new approach to model demands depending on their geographical location (network topology).

$$\boldsymbol{d}_i(t) = \frac{bd_i}{\sum_{j=1}^{n_d} bd_j} \cdot \boldsymbol{c_{j\rightarrow i}}(t) \cdot \boldsymbol{q_{in}}(t) \quad \text{(eq. 2.1.1)}$$

Where $\boldsymbol{c_{j\rightarrow i}}(t)$ is the value of the demand component *j* associated to node *i* depending on the node location. Demand components are calibrated demand multipliers that represent the behaviour of nodes in a determined geographical zone, avoiding dependency on information of user type and diurnal pattern behaviour. All nodes in the same area of node *i* have the same associated demand component. Consequently, all nodes in the same zone will have the same demand behaviour, weighted depending on their base demand. This demand model is capable of generating pressure variations in different zones of the network, as happens in a real situation. However, the assumption that all nodes in the same area behave exactly in the same way is not realistic. For example, a node within the limit of the effect zone of two demand components should probably have a combination of the behaviour of the two demand components instead of only one. To solve that, the demand model in equation 2.1.1 can be refined so that the level to which each demand component is associated with each node is given as a membership that depends on their geographical location. Equation 2.1.2 represents the new demand model.

$$\boldsymbol{d}_i(t) = \frac{bd_i}{\sum_{j=1}^{n_d} bd_j} \cdot \boldsymbol{q_{in}}(t) \cdot [\propto_{i,1} \cdot \boldsymbol{c}_1(t) + \propto_{i,2} \cdot \boldsymbol{c_2}(t) + \cdots + \propto_{i,n_c} \cdot \boldsymbol{c_{n_c}}(t)] \text{(eq. 2.1.2)}$$

With $\propto_{i,1} + \propto_{i,2} + \cdots + \propto_{i,n_c} = 1, \forall i$, where $\propto_{i,j}$ is the association of demand component *j* with node *i*; and n_c is the number of demand components. The membership of each node to each demand component depends on the geographical location of the node and is computed by means of a sensitivity analysis detailed in [11]. The model in equation 2.1.2 is capable of generating different behaviours in every demand, while only having to calibrate a few (n_c) demand components. The calibrated demand components generate individual demands that may not be exactly as the real ones, but the aggregated demand in a zone at a specific sample, and the cumulative demand of each individual node during a period of time (similar to the billing) will coincide with the real ones if other parameters (roughness, valve status, etc.) are well calibrated.

2.2 Leak Localisation

The leak localization method is based on comparing the monitored pressure variations caused by leaks at certain n_s inner nodes of the DMA network with the theoretical pressure variations caused by all potential leaks obtained using the DMA network mathematical model. Thereby, the residual set, $\boldsymbol{r} \in \Re^{n_s}$, is determined by the difference between the measured pressure at inner nodes, $\boldsymbol{p} \in \Re^{n_s}$, and the estimated pressure at these nodes obtained using the network model considering a leak-free scenario, $\widehat{\boldsymbol{p}}_{\boldsymbol{0}} \in \Re^{n_s}$:

$$\boldsymbol{r} = \boldsymbol{p} - \widehat{\boldsymbol{p}}_{\boldsymbol{0}} \quad (2.2.1)$$

Leaks **f** are assumed to be located in the nodes, this approximation is reasonable since the location accuracy exceeds the length of the pipes in a DMA. Thus, the number of potential leaks is considered to be equal to the number of network nodes *np*. The theoretical pressure disturbances caused by all potential leaks are stored in the theoretical fault signature matrix, $\boldsymbol{FSM} \in \Re^{n_s \times n_p}$. This matrix can be obtained from a sensitivity-to-leak analysis, as explained in [9]. It evaluates the theoretical effect of a potential leak f_j (in node j) on the pressure of each monitored node *I*, p_i, which

determine the theoretical residual vector $\boldsymbol{s}_j$. If this process is repeated for all potential leaks, the sensitivity matrix is obtained as:

$$\boldsymbol{S} = \begin{pmatrix} \frac{\partial p_1}{\partial f_1} & \cdots & \frac{\partial p_1}{\partial f_{np}} \\ \vdots & \ddots & \vdots \\ \frac{\partial p_{ns}}{\partial f_1} & \cdots & \frac{\partial p_{ns}}{\partial f_{np}} \end{pmatrix} \tag{2.2.2}$$

where each element s_{ij} measures the effect of the leak f_j in the pressure p_i of the node where the inner pressure sensor i is located. It is extremely difficult to calculate S analytically in a real network because a water network is a large scale problem described by a multivariable non-linear system of equations which may also be non-explicit. Thereby, the sensitivity matrix is generated by simulation of the network model approximating the sensitivity s_{ij} by

$$s_{ij} = \frac{\hat{p}_{if_j} - \hat{p}_{i0}}{f_j} \tag{2.2.3}$$

where $\hat{p}_{if_j}$ is the predicted pressure in the node where the pressure sensor i is placed when a nominal leak f_j is forced in node j and $\hat{p}_{i0}$ is the predicted pressure associated with the sensor i under a scenario free of leaks [6]. Then, repeating this process for all n_p potential faults the approximation of the sensitivity matrix is obtained. Vector (7) at a given time instant k is obtained a:

$$\boldsymbol{r}(k) = \begin{pmatrix} p_1(k) - \hat{p}_{10}(k) \\ \vdots \\ p_{ns}(k) - \hat{p}_{ns0}(k) \end{pmatrix} \tag{2.2.4}$$

The proposed leak location method is based on comparing the residual vector $\boldsymbol{r}$ in (2.2.1) with the theoretical fault signatures $\boldsymbol{s_i}$ of all potential leaks obtained from (2.2.2) using the approximation given by (2.2.3) and stored in the $\boldsymbol{FSM}$ matrix. This comparison is done by applying the correlation function

$$\rho_{\boldsymbol{s}_i,\boldsymbol{r}} = \mathrm{cov}(\boldsymbol{s}_i, \boldsymbol{r}) / \sqrt{\mathrm{cov}(\boldsymbol{s}_i, \boldsymbol{s}_i)\mathrm{cov}(\boldsymbol{r}, \boldsymbol{r})} \tag{2.2.5}$$

where $\mathrm{cov}(\boldsymbol{a}, \boldsymbol{b}) = E\left[(\boldsymbol{a} - \bar{a})(\boldsymbol{b} - \bar{b})\right]$ is the covariance function between two variables a and b, being $\bar{a} = E(\boldsymbol{a})$ and $\bar{b} = E(\boldsymbol{b})$, respectively. Those potential leaks whose theoretical signatures (columns of $\boldsymbol{FSM}$) have the highest correlation values with the residual vector $\boldsymbol{r}$ point out the most probable nodes to have the leak

$$\max_i \left(\rho_{s_i,r}\right) \quad , \quad i = 1,\ldots,np \tag{2.2.6}$$

where $\rho_{s_i,r}$ is the obtained correlation between the residual vector $\boldsymbol{r}$ and the ith–column of the theoretical fault signature matrix, $\boldsymbol{s}_i$, associated with a potential leak in node i. This methodology is developed thinking on real water distribution networks with kilometers of pipes. The consistency between measurements and model prediction is always difficult to achieve because of model uncertainty, especially in the nodal demands that usually are estimated. Thus, the detection phase is

usually treated in another level of supervision using DMA information regarding night flows and water balance performance.

3 RESULTS

Demand components from equation 2.1.2 are calibrated by solving the inverse problem using least squares minimization and the SVD to compute the inverse of the sensitivity matrix. Figure 2 depicts a grayscale map with the membership of each node to a particular demand component: the darker the node in the map, the higher the membership of the node to the demand component. The sensor with the highest sensitivity to variations in each demand component is also depicted in each map. Figure 3and Figure 4 depict the flow and pressure prediction errors for the calibration dataset. Each figure has two columns of subfigures, corresponding to the prediction error when using the basic demand model, and the prediction error when using the demand components model. Finally, Figure 6 presents the average percentage of consumption of each demand component, depending on the model used: the black line corresponds to the basic demand model (assumed demands from billing), and the green line with triangles corresponds to the demand components model.

It can be seen that the flow prediction error is reduced to irrelevant values, and that the pressure prediction error is considerably minimized in all sensors, except sensor RE38. This sensor is located near a pressure reduction valve (Figure 8), making the pressure modification more difficult. A detailed analysis is presented next. Figure 5shows a good accuracy in the average percentage of demand components consumption for components c1, c2, c3, and c5. Demand component c6 consumes more water than expected at the expense of demand component c4, which consumes less than expected. These two demand components are situated side by side, what could explain this behaviour. Besides, the proximity of sensor R38 (situated in the area predominated by component c6) to a network input could also explain this inaccuracy.

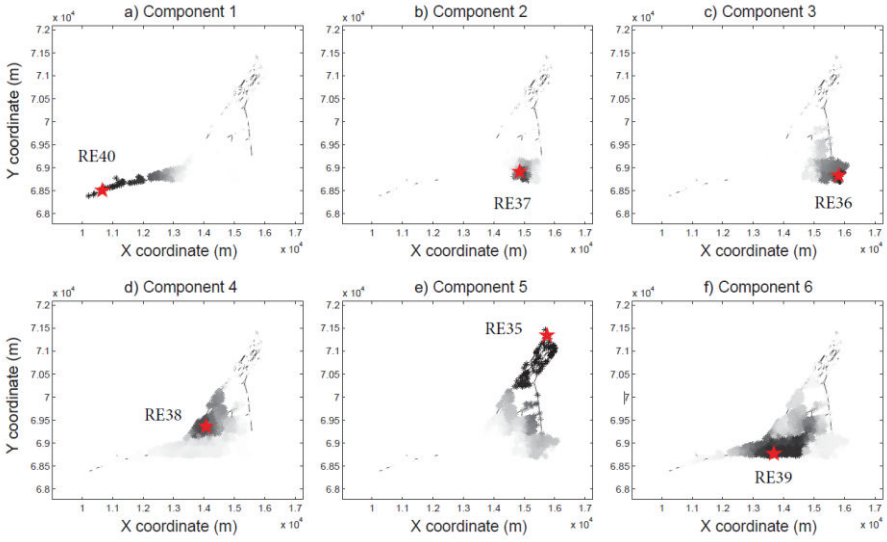

Figure 2: Memberships of nodes to each demand component in Castelldefels Platja network considering the six installed sensors (red stars).

The errors observed (pressure prediction and average percentage of consumption) related with the sensor RE38 have motivated an analysis of what may produce these inaccuracies. Sensor RE38 is situated near a network water input, where pressure is controlled by means of a PRV (Figure 7). The

proximity of the sensor to the point where pressure is fixed should make the measurement similar to this pressure and slightly affected by flow variations. However, as seen in Figure 7.a, the sensor measurement (green dots) varies its pressure depending on the global water consumption of the network (Figure 6.b).

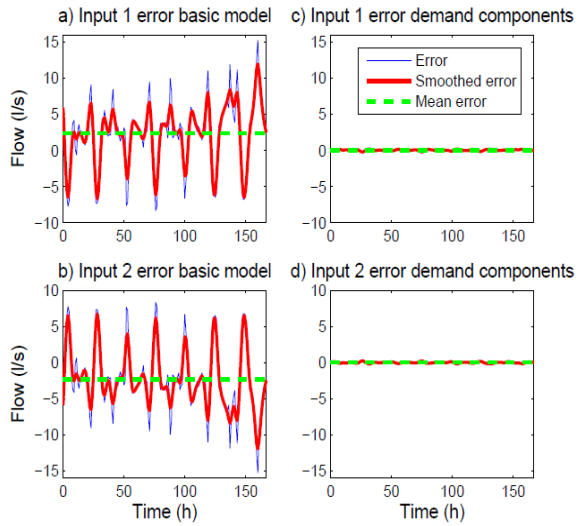

Figure 3: Flow prediction errors

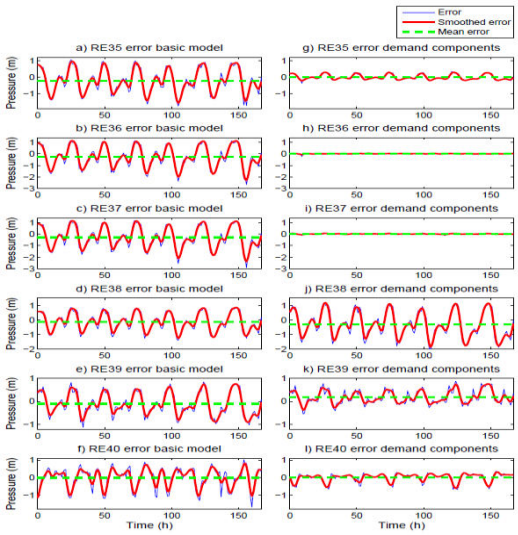

Figure 4: Pressure prediction errors

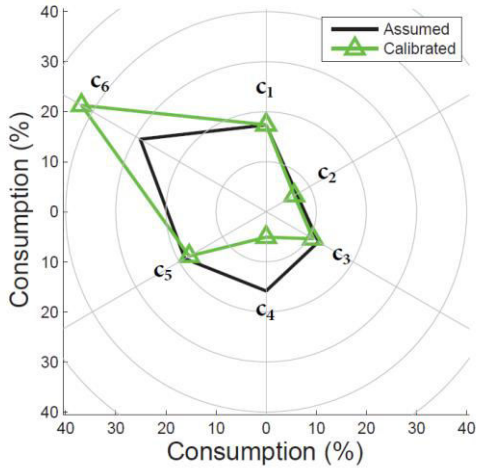

Figure 5: Percentage of consumption for each component (1rst calibration)

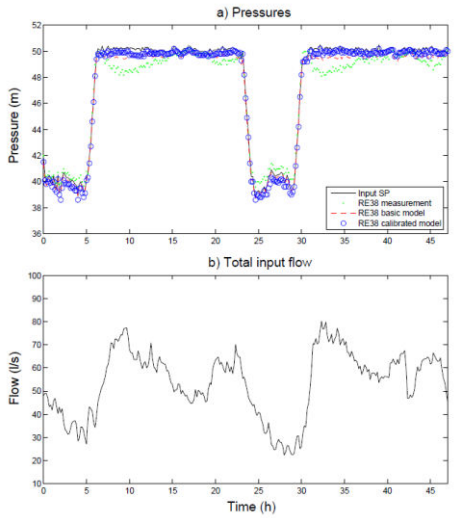

Figure 6: Pressure at input and sensor RE38 and total inflow

This behaviour is explained by the effect of head loss due to a long way from the fixed pressure point. On the other hand, both the sensor pressure prediction with the basic (red dashed line) and the calibrated (blue circles) demand models are nearly identical to the fixed pressure at the PRV (black line). In conclusion, the inaccuracies in the calibration results suggest a possible closed pipe between the area where sensor RE38 is located and the network input next to that area. The detection of this type of model structural errors is pointed out as an important factor for a good calibration in [16]. In Figure 9 the result of applying the leakage localization methodology (Section 2.2) using the corrected measurements registered during September 30th (day in which the forced leak was running the 24 hours) is presented. It shows the performance of leak localization method

highlighting the leak exact location (red star), the most correlated location predicted by the method (green star) and other locations (black spots) presenting also high correlations (> 99% of the highest correlation). The result presented in this figure is quite acceptable since the nodes with the highest probability to contain the leak (green and black dots) include the exact localization of the real leak in a small area. The nodes contained in this area have very similar pressure sensitivity to leak and as a consequence, inside, no leak can be isolated. The size of this area depends basically on the inner pressure sensor distribution computed by the optimal pressure sensor methodology [1]. In general, this is a trade-off between the number of inner pressure sensors and the resulting resolution of the leakage localization methodology. Then, applying the leakage localization methodology to the October 2nd registered data (Figure 10), it can be seen that the probability to contain the leak of the nodes with the highest probabilities (green and black dots) have very small values (around 0.16 being 1 the maximum value). This is normal since the real leak is already over but additionally, this confirms that the highest probability values obtained in the September 30th analysis (around 0.65 being 1 the maximum value) (leak running the 24 hour) are basically due to effect of the leak on the pressure registered by the sensors. The reasons for not obtaining higher probabilities in 30th September analysis are basically due to the effect of the remaining modelling uncertainty/errors.

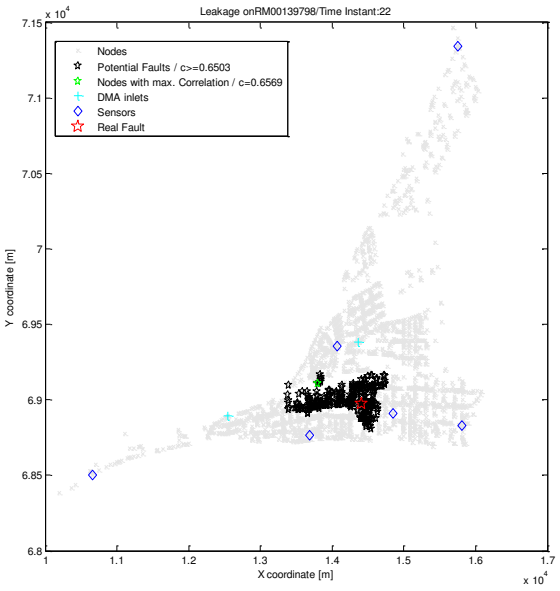

Figure 9: Performance of leak localization method (September 30th)

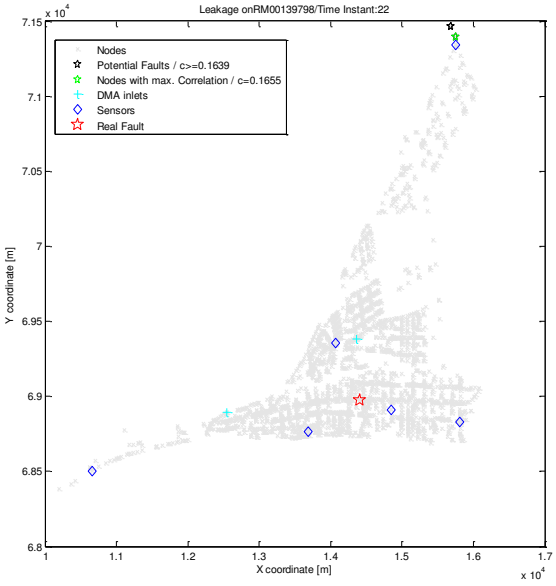

Figure 10: Performance of leak localization method (October 2nd)

4 CONCLUSIONS

The leak localisation methodology applied in this work had given already good results in synthetic data based on simulation. The deterioration of its performance when applied to real data had been already identified with problems in the modelling. In the present work an ambitious challenge of localising a leak in a huge DMA was stated in order to test the improvement produced by the demand calibration. The difficulties of the demand calibration methodology were first a setback that became a side utility of the methodology when allowed to identify a topologic error in the model. Finally, the results improve notoriously when the model is adjusted both topologically and in demands. The good results when the models are applied, for leak localisation in this case, is a

proper approach of validation as no model is useful for everything and they have to be evaluated in their final purpose.

5 ACKNOWLEGMENTS

This work has been funded by the Spanish Ministry of Economy and Competitiveness (MINECO) and FEDER through the projects ECOCIS (ref. DPI2013-48243-C2-1-R) and HARCRICS (ref. DPI2014-58104-R).

References

[1] Bonada et al., 2014. Practical-Oriented Pressure Sensor Placement for Model-based Leakage Location in Water Distribution Networks. 11th International Conference on Hydroinformatics.

[2] Goldberg, D.E., 1989. Genetic Algorithms in Search, Optimization, and Machine Learning. Addison-Wesley, Reading, MA

[3] Kang, D. & Lansey, K., 2011. Demand and Roughness Estimation in Water Distribution Systems. Journal of Water Resources Planning and Management, 137(1), pp.20–30.

[4] Maier, H.R. et al., 2014. Evolutionary algorithms and other metaheuristics in water resources: Current status, research challenges and future directions. Environmental Modelling & Software, 62, pp.271–299.

[5] Meseguer, J. et al., 2015. Model-based Monitoring Techniques for Leakage Localization in Distribution Water Networks. Computing and Control for the Water Industry (CCWI2015). Procedia Engineering, Volume 119, 2015, Pages 1399-1408, ISSN 1877-7058

[6] Pérez, R. et al., 2014. Leak Localization in Water Networks: A Model-Based Methodology Using Pressure Sensors Applied to a Real Network in Barcelona [Applications of Control]. IEEE Control Systems, 34(4), pp.24–36.

[7] Pérez, R., Sanz, G., Quevedo, J., Nejjari, F., Meseguer, J., Cembrano, G., y otros. (2014). Leak Localization in Water Networks. IEEE CONTROL SYSTEMS MAGAZINE, 24-36.

[8] Pérez, R. et al., 2011. Methodology for leakage isolation using pressure sensitivity analysis in water distribution networks. Control Engineering Practice, 19(10), pp.1157–1167.

[9] Pudar, R. S., & Liggett, J. A. (1992). Leaks in Pipe Networks. Journal of Hydraulic Engineering, 118(7), 1031–1046.

[10] Puust, R. et al., 2010. A review of methods for leakage management in pipe networks. Urban Water Journal, 7(1), pp.25–45.

[11] Sanz, G. & Pérez, R., 2015. Sensitivity Analysis for Sampling Design and Demand Calibration in Water Distribution Networks Using the Singular Value Decomposition. Journal of Water Resources Planning and Management, p.04015020.

[12] Savic, D., Kapelan, Z. & Jonkergouw, P., 2009. Quo vadis water distribution model calibration? Urban Water Journal, 6(1), pp.3–22.

[13] Sumer, D. & Lansey, K., 2009. Effect of Uncertainty on Water Distribution System Model Design Decisions. Journal of Water Resources Planning and Management, 135(1), pp.38–47.

[14] van Thienen, P., 2013. A method for quantitative discrimination in flow pattern evolution of water distribution supply areas with interpretation in terms of demand and leakage. Journal of Hydroinformatics, 15(1), p.86.

[15] Vítkovský, J., Simpson, A. & Lambert, M., 2000. Leak Detection and Calibration Using Transients and Genetic Algorithms. Journal of Water Resources Planning and Management, 126(4), pp.262–265.

[16] T. Walski, P. Sage, and Z. Wu. What Does it Take to Make Automated Calibration Find Closed Valves and Leaks? World Environmental and Water Resources Congress 2014, pages 555-565, 2014.